Draft version April 12, 2017
Typeset using LaTeX **modern** style in AASTeX61

DISTINGUISHING SPIN-ALIGNED AND ISOTROPIC BLACK HOLE POPULATIONS WITH GRAVITATIONAL WAVES

Will M. Farr,[1] Simon Stevenson,[1,2] M. Coleman Miller,[3] Ilya Mandel,[1,2]
Ben Farr,[4] and Alberto Vecchio[1]

[1] *Birmingham Institute for Gravitational Wave Astronomy and School of Physics and Astronomy, University of Birmingham, Birmingham, B15 2TT, United Kingdom*
[2] *Kavli Institute for Theoretical Physics, Santa Barbara, CA 93106*
[3] *Department of Astronomy and Joint Space-Science Institute, University of Maryland, College Park, MD 20742–2421, United States*
[4] *Enrico Fermi Institute and Kavli Institute for Cosmological Physics, University of Chicago, Chicago, IL 60637, United States*

ABSTRACT

The first direct detections of gravitational waves (GWs) from merging binary black holes (BBHs) open a unique window into the BBH formation environment. One promising signature of the formation environment is the angular distribution of the black hole (BH) spins; systems formed through dynamical interactions among already-compact objects are expected to have isotropic spin orientations whereas binaries formed from pairs of stars born together are more likely to have spins preferentially aligned with the binary orbit as a consequence of their joint evolution toward a BBH system. We consider existing GW measurements of $\chi_{\rm eff}$, the best-measured combination of spin parameters, in the three likely binary black hole detections GW150914, LVT151012, and GW151226. If binary black hole spin magnitudes extend to high values, as is suggested by observations of black hole X-ray binaries, we show that the data already exhibit a 1.7σ (0.087 odds ratio[a)]) preference for an isotropic angular distribution. By considering the effect of an additional 10 detections drawn from the various models in the suite we show that if all observations come from a single population such an augmented data set would enable at least a 2.9σ (0.0035 odds ratio) distinction between the isotropic and aligned models for the assumed spin magnitude distributions, and in most cases better than 5σ (2.9×10^{-7} odds ratio). The existing preference for either an isotropic spin distribution or low spin magnitudes for the observed systems will be confirmed (or overturned) confidently in the near future by

w.farr@bham.ac.uk, simons@star.sr.bham.ac.uk, miller@astro.umd.edu,
imandel@star.sr.bham.ac.uk, farr@uchicago.edu, av@star.sr.bham.ac.uk

a) An odds ratio of r with $r \ll 1$ is equivalent to $x\sigma$ with $x = \Phi^{-1}(1 - r/2)$, where Φ is the unit normal CDF.

subsequent observations.

1. GW SPIN MEASUREMENTS AND MODEL SELECTION

Following the detection of a merging binary black hole (BBH) system, parameter estimation (PE) tools (Veitch et al. 2015) compare model gravitational waveforms (e.g. Pan et al. 2014; Taracchini et al. 2014; Hannam et al. 2014) against the observed data to obtain a posterior distribution on the parameters that describe the compact binary source.

The spin parameter with the largest effect on waveforms, and a correspondingly tight constraint from the data, is a mass-weighted, aligned, "effective spin,"

$$\chi_{\rm eff} = \frac{c}{GM}\left(\frac{\vec{S}_1}{m_1} + \frac{\vec{S}_2}{m_2}\right)\cdot\frac{\vec{L}}{\left|\vec{L}\right|} \equiv \frac{1}{M}\left(m_1\chi_1 + m_2\chi_2\right), \tag{1}$$

where $m_{1,2}$ are the gravitational masses of the more-massive (1) and less-massive (2) components, $M = m_1 + m_2$ is the total mass, $\vec{S}_{1,2}$ are the spin angular momentum vectors of the black holes in the binary, $\vec{L}$ is the orbital angular momentum vector, assumed to point in the $\hat{z}$ direction, and $0 \leq \chi_{1,2} \leq 1$ are the corresponding dimensionless projections of the individual black hole (BH) spins (Abbott et al. 2016a).

Figure 1 shows an approximation to the posterior inferred on $\chi_{\rm eff}$ for the three likely GW detections GW150914, GW151226 and LVT151012 from Advanced LIGO's first observing run (O1) (Abbott et al. 2016b). Because samples drawn from the posterior on $\chi_{\rm eff}$ are not publicly released at this time, we have approximated the posterior as a Gaussian distribution with the same mean and 90% credible interval as quoted in Abbott et al. (2016b). None of the $\chi_{\rm eff}$ posteriors are consistent with two black holes with large aligned spins, $\chi_{1,2} \gtrsim 0.5$; this contrasts with the large spins inferred for the majority of black holes in X-ray binaries (see Section 2). ~~Since all three mergers involve black holes of comparable masses, there is essentially no posterior support for both black holes' $\chi \gtrsim 0.5$, in contrast to the majority of the electromagnetically-detected stellar-mass black hole population (see Section 2).~~ The analysis here is relatively insensitive to the precise details of the posterior distributions; other conclusions are more sensitive. In particular, our Gaussian approximation does permit $\chi_{\rm eff} = 0$ for GW151226 while the true posterior rules this out at high confidence (Abbott et al. 2016c,b).

Small values of $\chi_{\rm eff}$ as exhibited in these systems can result from either intrinsically small spins or larger spins whose direction is mis-aligned with the orbital angular momentum of the binary (i.e. spin vectors with small z-components). Mis-alignment is capable of producing *negative* values of $\chi_{\rm eff}$, however, whereas aligned spins will always have $\chi_{\rm eff} \geq 0$. This difference provides strong discriminating power between the two angular distributions, even without good information about the magnitude distribution; to the extent that data favour negative $\chi_{\rm eff}$ they weigh heavily against aligned models. To quantify the degree of support for these two alternate explanations of small $\chi_{\rm eff}$ values in the merging BBH population, we compared the Bayesian evidence for various simple models of the spin population using the GW data set.

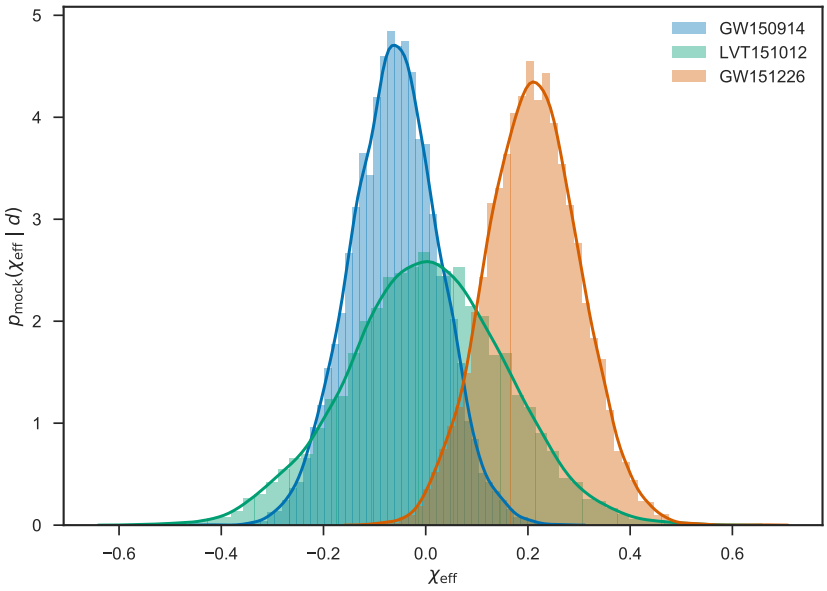

Figure 1. Approximate posteriors on χ_{eff} from the Advanced LIGO O1 run observations in Abbott et al. (2016b). We approximate the posteriors reported in Abbott et al. (2016b) using Gaussians with the same median and 90% credible interval as reported in Abbott et al. (2016b). It is notable that none of the χ_{eff} posteriors supports high BH spin magnitudes with aligned spins, suggested by observations of stellar-mass black holes in X-ray binaries (see Miller & Miller (2015) for a summary of such measurements).

Each of our models for the merging BBH spin population assumes that the merging black holes are of equal mass (this is marginally consistent with the three observations (Abbott et al. 2016b), and the χ_{eff} distribution is not particularly sensitive to the mass ratio between the merging objects—see Section D). We assume that the population spin distribution factorises into a distribution for the spin magnitude a and a distribution for the spin angles. Finally, we assume that the distribution of spins is common to each component in a merging binary. Choosing one of three magnitude distributions

$$p(a) = \begin{cases} 2\,(1-a) & \text{“low”} \\ 1 & \text{“flat”} \\ 2a & \text{“high”} \end{cases}, \tag{2}$$

and pairing with either an isotropic angular distribution or a distribution that generates perfect alignment with the positive z axis yields six different models for the χ_{eff} distribution. These models are shown in Figure 2.

The distributions in Eq. (2) are not meant to represent any particular physical model, but rather to capture our uncertainty about the spin magnitude distribution, discussed in detail in Section 2; neither observations nor population synthesis codes can at this point authoritatively suggest *any* particular spin distribution (Miller &

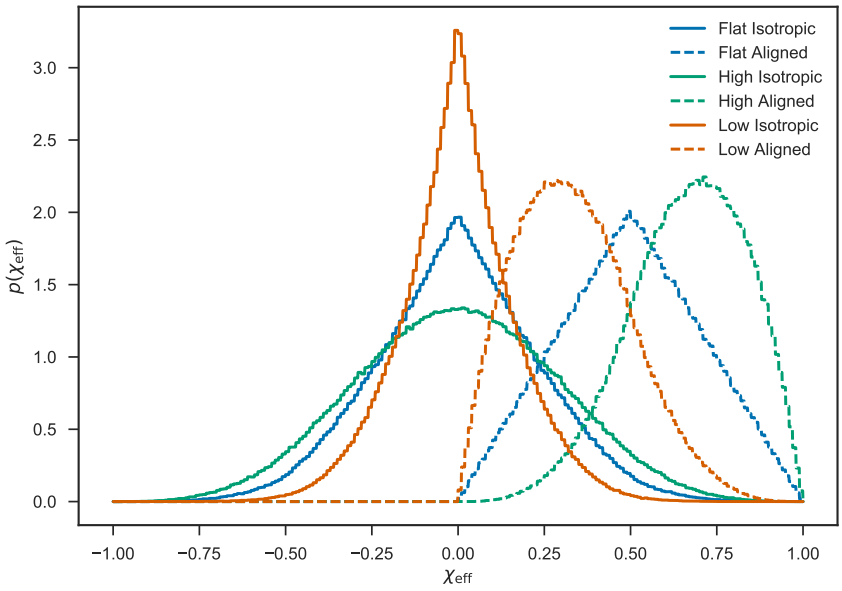

Figure 2. The models for the distribution of $\chi_{\rm eff}$ considered in this paper. In all models we assume that the binary mass ratio $q \equiv m_1/m_2 = 1$ and that the distribution of spin vectors is the same for each component. The "flat" (blue lines), "high," (green lines), and "low" (red lines) magnitude distributions are defined in Eq. (2). Solid lines give the $\chi_{\rm eff}$ distribution under the assumption that the orientations of the spins are isotropic; dashed lines give the distribution under the assumption that both objects' spins are aligned with the orbital angular momentum. The isotropic distributions are readily distinguished from the aligned distributions by the production of negative $\chi_{\rm eff}$ values, while the distinction between the three models for the spin magnitude distribution is less sharp.

Miller 2015). Our models, however, allow us to see how sensitive the $\chi_{\rm eff}$ distribution is to spin alignment given uncertainties about the spin magnitudes.

We fit hierarchical models of the three LIGO O1 observations using these six different, zero-parameter population distributions (see Section B). We also fit three mixture models for the population, where the spin magnitude distribution is fixed but the angular distribution is a weighted sum of the isotropic and aligned distribution. The evidence, or marginal likelihood, for each of the models is shown in Figure 3. For all three magnitude distributions, the mixture models' posterior on the mixing fraction peaks at 100% isotropic, which explains why the zero-parameter, pure-isotropic models are preferred over the single-parameter mixture models for every magnitude distribution with this data set. Not surprisingly, given the small $\chi_{\rm eff}$ values in the three detected systems, the most-favoured model among those with an isotropic angular distribution has the "low" magnitude distribution; the most favoured model among those with an aligned distribution also has the "low" magnitude distribution. The odds ratio between the "low" aligned and "low" isotropic models is 0.087, or 1.7σ; thus the data favour isotropic spins among our suite of models. While the data favour spin amplitude distributions with small spin magnitudes, note that a model

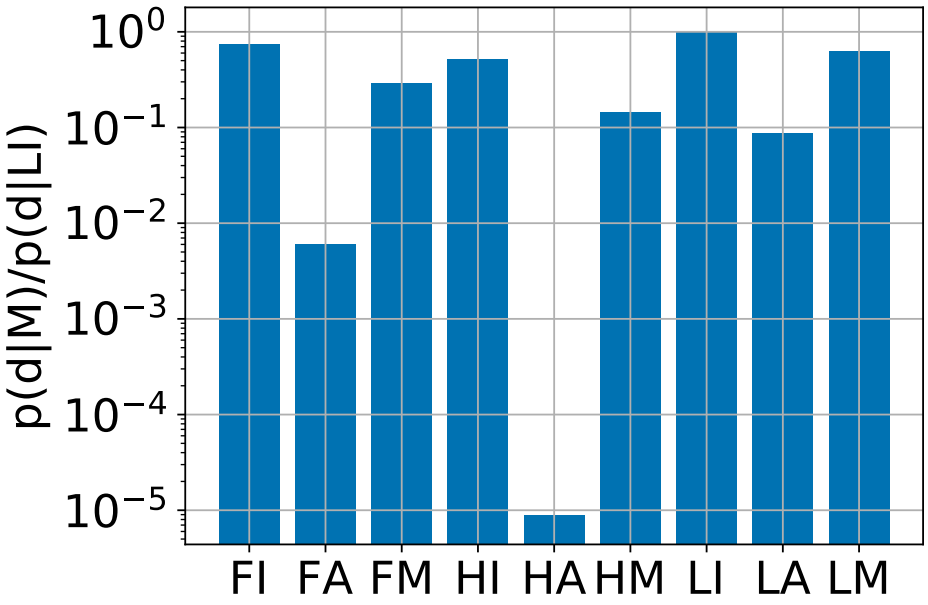

Figure 3. Odds ratios among our models using the approximations to the posteriors on $\chi_{\rm eff}$ from the O1 observations shown in Figure 1. The flat ("F"), high ("H"), and low ("L") spin magnitude distributions (see Eq. (2)) are paired with isotropic ("I") and aligned ("A") angular distributions, as well as a mixture model of the two ("M"). The most-favoured models have the "low" distribution of spin magnitudes. The odds ratio between these models is 0.087, or 1.7σ. For all magnitude distributions the pure-isotropic models are preferred over the mixture models; correspondingly, the posterior on the mixture fraction peaks at 100% isotropic.

with all BBH systems having zero spin is ruled out by the GW151226 measurements, which bound at least one black hole to have spin magnitude ≥ 0.2 at 90% credibility (Abbott et al. 2016c).

1.1. *Future Spin Measurements*

Estimates of the rate of BBH coalescences give a reasonable chance of 10 additional BBH detections in the next two years (Abbott et al. 2016b,d,e). Assuming 10 additional detections with similar observational uncertainties [I think it would be useful to specify (in an appendix?) what model we use for the observational uncertainty on $\chi_{\rm eff}$.] drawn from each of our six zero-parameter models for the spin distribution in addition to the three existing detections from O1, we find the odds ratios shown in Figure 4. We find that most scenarios with an additional 10 detections allow the simulated angular distribution to be inferred with greater than 5σ (2.9×10^{-7} odds) credibility; and in the most pessimistic case the distinction is typically 2.9σ (0.0035 odds ratio). While such future detections should permit a confident distinction between *angular* distributions, we would remain much less certain about the *magnitude* distribution among the three options considered here until we have a larger number of observations. In Figure 4, the odds ratio between different magnitude distribu-

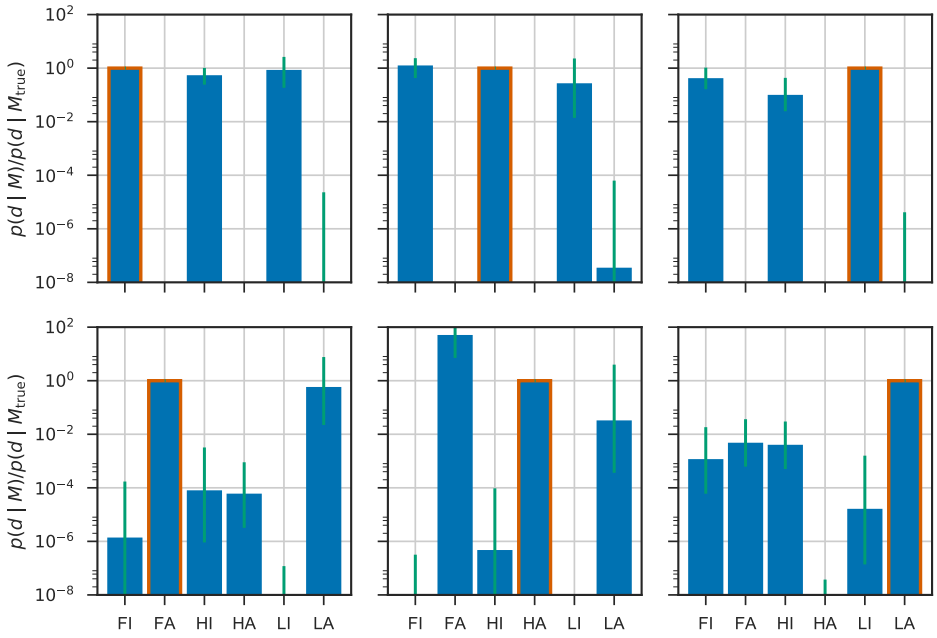

Figure 4. Distribution of odds ratios predicted with 10 additional observations above the three discussed in Section 1. Each panel corresponds to additional observations drawn from one of the $\chi_{\rm eff}$ distribution models. The model from which the additional observations are drawn is outlined in red. The height of the blue bar gives the median odds ratio relative to the model from which the additional observations are drawn; the green line gives the 68% (1σ) symmetric interval of odds ratios over 1000 separate draws from the model distribution. The closest median ratio between the most-favoured isotropic model and the most-favoured aligned model is 0.0035, corresponding to 2.9σ preference for the correct angular distribution; most models result in more than 5σ preference for the correct angular distribution. Because the three observations from Section 1 are included in each data set the "correct" model is not necessarily preferred over the others, particularly when that model uses the "high" magnitude distribution, which is strongly dis-favoured from the O1 observations alone.

tions with the same angular distribution is much closer to unity than the odds ratio between angular distributions.

2. DISCUSSION

Most of our resolving power for the spin angular distribution is a result of the fact that our "aligned" models cannot produce $\chi_{\rm eff} < 0$ (see Figure 2). If spins are intrinsically very small, with $a \lesssim 0.3$, then it is no longer possible to resolve the negative effective spin with a small number of observations. As noted below, however, spins observed in X-ray binaries are typically large. Additionally, models which do not permit *some* spins with $\chi_{\rm eff} \gtrsim 0.1$ are ruled out by the GW151226 observations (Abbott et al. 2016c).

In order to perform our analysis we need to select models for the distribution of the spin magnitudes of stellar-mass black holes. Observational data for such model selection is sparse. Miller & Miller (2015) give current estimates of the spin parameters for stellar-mass black holes, obtained using disk reflection and/or disk continuum

methods. Most of the systems studied are low-mass X-ray binaries rather than the high-mass X-ray binaries that are likely to be the progenitors of double black hole binaries. In addition, there are substantial systematic errors that can complicate either type of analysis (see Miller & Miller 2015 for a discussion), and selection effects could yield a biased distribution. Nonetheless, if we take the reported spin magnitudes as representative then we find that there is a preference for high spins; for example, 14 of the 19 systems with reported spins have dimensionless spin parameters in excess of 0.5. It is usually argued that the masses and spin parameters of stellar-mass black holes are unlikely to be altered significantly by accretion (low-mass donors may not have enough mass and high-mass donors have a very short phase in which they transfer mass; a variant of this long-standing argument was presented by King & Kolb (1999)), but see Podsiadlowski et al. (2003); Fragos & McClintock (2015). Thus the current spin parameters probably are close to their values upon core collapse, at least in high-mass X-ray binaries. However, the specific processes involved in the production of black hole binaries from isolated binaries could alter the spin magnitude distribution of those holes relative to the X-ray binary systems; for example, close tidal interactions could spin up the core, or stripping of the envelope could reduce the available angular momentum (Kushnir et al. 2016; Zaldarriaga et al. 2017; Hotokezaka & Piran 2017).

The spin directions of binary black holes formed dynamically through interactions in dense stellar environments (Sigurdsson & Hernquist 1993; Kulkarni et al. 1993; Portegies Zwart & McMillan 2000; Rodriguez et al. 2015; Stone et al. 2017) are expected to be isotropic given the absence of a preferred direction (e.g., Rodriguez et al. 2016) and the persistence of an isotropic distribution through post-Newtonian evolution (Schnittman 2004; Bogdanović et al. 2007).

The spin directions in isolated binaries, whether evolving via the classical channel through a common-envelope phase (Tutukov & Yungelson 1973; Tutukov & Yungelson 1993; Lipunov et al. 1997; Belczynski et al. 2016; Stevenson et al. 2017b) or through chemically homogeneous evolution (Mandel & de Mink 2016; Marchant et al. 2016) are usually expected to be preferentially aligned. Despite observed spin-orbit misalignments in both massive stellar binaries (Albrecht et al. 2009, 2014) and BH X-ray binaries (Orosz et al. 2001; Martin et al. 2008a,b; Morningstar & Miller 2014), mass accretion and tidal interactions will tend to realign the binary. On the other hand, a supernova natal kick (if any) can change the orbital plane and misalign the binary (Kalogera 2000; Gerosa et al. 2013); the supernova can also tilt the spin angle, as in the double pulsar J0737-3039 (Farr et al. 2011); and a variety of uncertain processes, such as wind-driven mass loss and post-collapse fallback, can couple the spin magnitude and direction distributions, contrary to our simplified assumptions. A small misalignment at wide separation can also evolve to a more significant misalignment in component spins as the binary spirals in through GW emission (Gerosa et al. 2015), but $\chi_{\rm eff}$ is approximately conserved through this evolution.

Vitale et al. (2017) also studied the possibility of distinguishing aligned and isotropic angular distributions of BBH spins, but concluded that several hundred sources would be required to adequately separate models which included both parallel and anti-parallel spins for an "aligned" population. In contrast, and in agreement with the present study, Stevenson et al. (2017a) found that only ~ 5 observations of rapidly spinning black holes would be necessary to distinguish isotropic and aligned spin distributions, though tens of detections would be required for more nuanced admixture models. Meanwhile, recent studies by Fishbach et al. (2017) and Gerosa & Berti (2017) focused on inference on spin magnitudes.

In summary, the angular distribution of spins in BBHs formed through isolated binary evolution is uncertain; nevertheless, it is more probable that spins are preferentially aligned after evolution through this channel than not, while an isotropic distribution of spins is the natural outcome of dynamical formation processes. Therefore, if the current observational trend for low $\chi_{\rm eff}$ continues with future gravitational-wave observations, it will be possible to either confirm that BH spins are isotropic in direction and sometimes large in magnitude, yielding a strong indication of a dynamical formation origin; or that BH spins are overwhelmingly small in magnitude, yielding a notable contradiction with the claimed BH X-ray binary spin measurements, particularly those for high-mass X-ray binaries.

We thank Richard O'Shaughnessy, Christopher Berry, and Davide Gerosa for discussions and comments on this work. WF, SS, IM and AV were supported in part by the STFC. MCM acknowledges support of the University of Birmingham Institute for Advanced Study Distinguished Visiting Fellows program. SS and IM acknowledge support from the National Science Foundation under Grant No. NSF PHY11-25915.

APPENDIX

A. MIXTURE MODEL

While we carried out Bayesian comparisons between isotropic and aligned spin distributions under various assumptions, a preference for one of the considered models over the others does not necessarily indicate that it is the correct model. All of the considered models could be inaccurate for the actual distribution, especially since all of the considered models are based on a number of additional assumptions, such as decoupled spin magnitude and spin misalignment angle distributions and identical distributions for primary and secondary spins.

We now partly relax the simplified assumptions made earlier by considering the possibility that the true distribution of BBH spin-orbit misalignments observed by LIGO is a mixture of binaries with aligned spins and binaries with isotropic spins.

Following Stevenson et al. (2017a), we fit a mixture model (labelled model 'M' in Figure 3) where a fraction f_i of BBHs have spins drawn from an isotropic distribution, whilst a fraction $1 - f_i$ have their spins aligned with the orbital angular momentum.

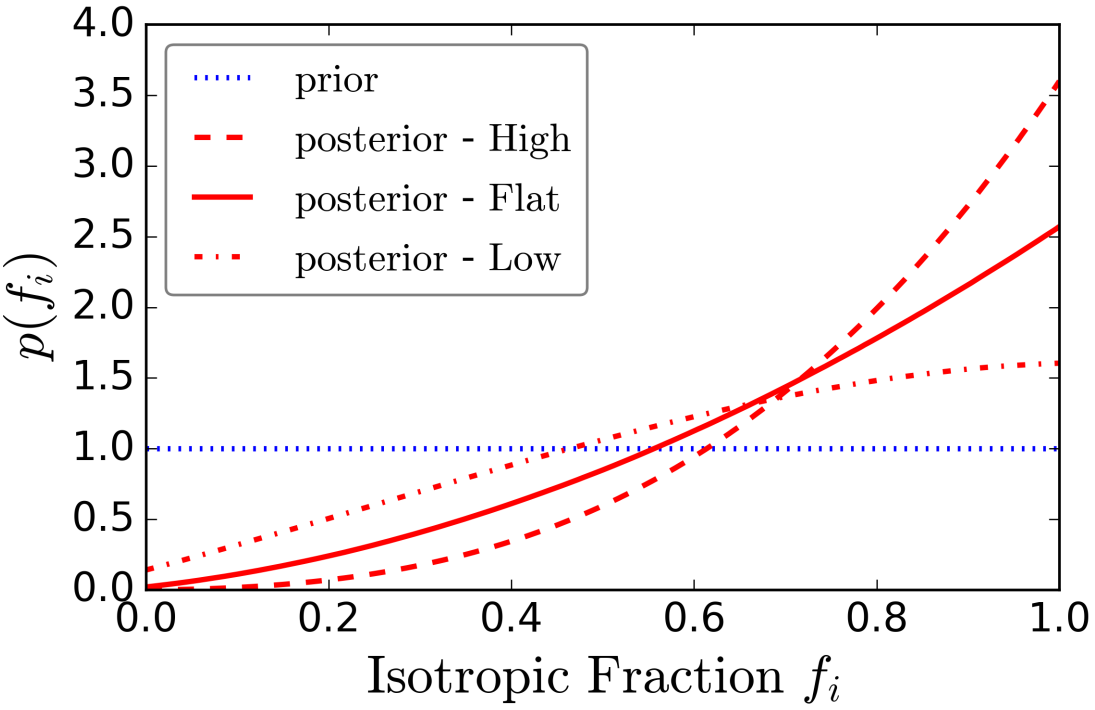

Figure 5. Fraction of the BBH population coming from an isotropic distribution under a mixture model. The dotted line shows the flat prior on the fraction of BBHs coming from an isotropic distribution, f_i, under the mixture model. The 3 red lines show the posterior on f_i after O1 with our various assumptions regarding BH spin magnitudes. The solid line shows the posterior assuming that all BHs have their spin magnitude drawn from the "flat" distribution. The dashed line assumes the "high" BH spin magnitude distribution $p(a) = 2a$. The dot-dash line assumes the "low" distribution $p(a) = 2(1-a)$. We see that for a wide range of assumptions regarding BH spin magnitudes, the fraction coming from an isotropic distribution f_i peaks at 1.

We assume a flat prior on the fraction f_i. To test the robustness of our result, we vary the distribution we assume for BH spin magnitude distributions as with the aligned and isotropic models. We use the "flat", "high" and "low" distributions (Equation 2), assuming all BHs have their spin magnitude drawn from the same distribution for both the aligned and isotropic populations. We calculate and plot the posterior on f_i given by Equation B3 ($f_i = \lambda$ in the derivation) in Figure 5. We find the mean fraction of BBHs coming from an isotropic distribution is 0.63, 0.71 and 0.78 assuming the "low", "flat" and "high" distributions for spin magnitudes respectively, compared to the prior mean of 0.5. The lower 90% limits are 0.26, 0.39 and 0.52 respectively, compared to the prior of 0.1. In all cases, the posterior peaks at $f_i = 1$. Thus, for these spin magnitude distributions we find that the current O1 LIGO observations constrain the majority of BBHs to have their spins drawn from an isotropic distribution. The evidence ratios of these models to the isotropic distribution with "flat" spin magnitudes are 0.85, 0.39 and 0.19 for the "low", "flat"

and "high" spin magnitude models. Thus we cannot rule out a mixture with the current data.

B. HIERARCHICAL MODELLING

LIGO measures $\chi_{\rm eff}$ better than any other spin parameter, but still with significant uncertainty, so we need to properly incorporate measurement uncertainty in our analysis; thus our analysis must be *hierarchical* (Hogg et al. 2010; Mandel 2010). In a hierarchical analysis, we assume that each event has a true, but unknown, value of the effective spin, drawn from the population distribution, which may have some parameters λ; then the system is observed, represented by the likelihood function, which results in a distribution for the true effective spin (and all other parameters describing the system) consistent with the data. Combining, the joint posterior on each system's $\chi^i_{\rm eff}$ parameters and the population parameters λ implied by a set of observations each with data d^i, is

$$p\left(\left\{\chi^i_{\rm eff}\right\},\lambda \mid \left\{d^i\right\}\right) \propto \left[\prod_{i=1}^{N_{\rm obs}} p\left(d^i \mid \chi^i_{\rm eff}\right) p\left(\chi^i_{\rm eff} \mid \lambda\right)\right] p\left(\lambda\right). \tag{B1}$$

The components of this formula are

- The GW (marginal) likelihood, $p\left(d \mid \chi_{\rm eff}\right)$. Here we use "marginal" because we are (implicitly) integrating over all parameters of the signal but $\chi_{\rm eff}$. Note that it is the likelihood rather than the posterior that matters for the hierarchical analysis; if we are given posterior distributions or posterior samples, we need to re-weight to "remove" the prior and obtain the likelihood.
- The population distribution for $\chi_{\rm eff}$, $p\left(\chi_{\rm eff} \mid \lambda\right)$. This function can be parameterised by population-level parameters, λ. (In the cases discussed above, there are no parameters for the population.)
- The prior on the population-level parameters, $p(\lambda)$.

If we do not care about the individual event $\chi_{\rm eff}$ parameters, we can integrate them out, obtaining

$$p\left(\lambda \mid \left\{d^i\right\}\right) \propto \left[\prod_{i=1}^{N_{\rm obs}} \int {\rm d}\chi^i_{\rm eff}\, p\left(d^i \mid \chi^i_{\rm eff}\right) p\left(\chi^i_{\rm eff} \mid \lambda\right)\right] p\left(\lambda\right). \tag{B2}$$

If we are given posterior samples of $\chi^{ij}_{\rm eff}$ (i labels the event, j labels the particular posterior sample) drawn from an analysis using a prior $p\left(\chi_{\rm eff}\right)$, then we can approximate the integral by a re-weighted average of the population distribution over the samples (here $p\left(\chi^{ij}_{\rm eff}\right)$ is the prior used to produce the posterior samples):

$$p\left(\lambda \mid \left\{d^i\right\}\right) \propto \left[\prod_{i=1}^{N_{\rm obs}} \frac{1}{N_i} \sum_{j=1}^{N_i} \frac{p\left(\chi^{ij}_{\rm eff} \mid \lambda\right)}{p\left(\chi^{ij}_{\rm eff}\right)}\right] p\left(\lambda\right). \tag{B3}$$

B.1. *Order of Magnitude Calculation*

It is possible to estimate at an order-of-magnitude level the rate at which evidence accumulates in favour of or against the isotropic models as more systems are detected. Based on Figure 2, approximate the isotropic population $\chi_{\rm eff}$ distribution as uniform on $\chi_{\rm eff} \in [-0.25, 0.25]$ and the aligned population $\chi_{\rm eff}$ distribution as uniform on $\chi_{\rm eff} \in [0, 0.5]$. Then the odds ratio between the isotropic and aligned models for each event is approximately

$$\frac{p\left(d \mid I\right)}{p\left(d \mid A\right)} \simeq \frac{P\left(-0.25 \leq \chi_{\rm eff} \leq 0.25\right)}{P\left(0 \leq \chi_{\rm eff} \leq 0.5\right)}, \tag{B4}$$

where $P\left(A \leq \chi_{\rm eff} \leq B\right)$ is the posterior probability (here used to approximate the likelihood) that $\chi_{\rm eff}$ is between A and B. Using our approximations to the $\chi_{\rm eff}$ posteriors described above, this gives an odds ratio of 5 in favour of the isotropic models, which is about a factor of two smaller than the ratio in the more careful calculation described in Section 1. This is a satisfactory answer at an order-of-magnitude level.

If the true distribution is isotropic and follows this simple model, and our measurement uncertainties on $\chi_{\rm eff}$ are $\simeq 0.1$, then the geometric mean of each subsequent measurement's contribution to the overall odds is ~ 3. After ten additional events, then, the odds ratio becomes $5 \times 3^{10} \simeq 3 \times 10^5$, or 4.6σ, consistent with the results of the more detailed calculation described above. If the true distribution of spins becomes half as wide ($\chi_{\rm eff} \in [-0.125, 0.125]$ for isotropic and $\chi_{\rm eff} \in [0, 0.25]$ for aligned spins), with the same uncertainties, then the existing odds ratio becomes 1.08, and each subsequent event drawn from the isotropic distribution contributes on average a factor of 1.6. In this case, after 10 additional events, the odds ratio becomes 150, or 2.7σ. With small spin magnitudes, our angular resolving power vanishes, as discussed in more detail in Section C.

C. EFFECT OF SMALL SPIN MAGNITUDES

In the main text we considered three models for BH spin magnitudes: "low", "flat" and "high". These were intended to capture some of the uncertainty regarding the BH spin magnitude distribution.

Here we extend the "low" model as:

$$p(a) \propto (1-a)^{\alpha} \tag{C5}$$

When $\alpha = 0$, this recovers the "flat" distribution, whilst $\alpha = 1$ recovers the "low" distribution. For higher values of α, this distribution becomes more peaked towards $a = 0$.

In Figure 6 we plot the evidence ratio of aligned to isotropic distributions (plotted as the equivalent sigma) with spin magnitudes given by this model with α in the range 0 – 6. The top axis shows the mean spin magnitude that value of α corresponds to (e.g., for the "flat" distribution $\alpha = 0$, the mean spin magnitude is 0.5). We see that if typical BH spins are $\lesssim 0.2$ we have no evidence for one model over the other.

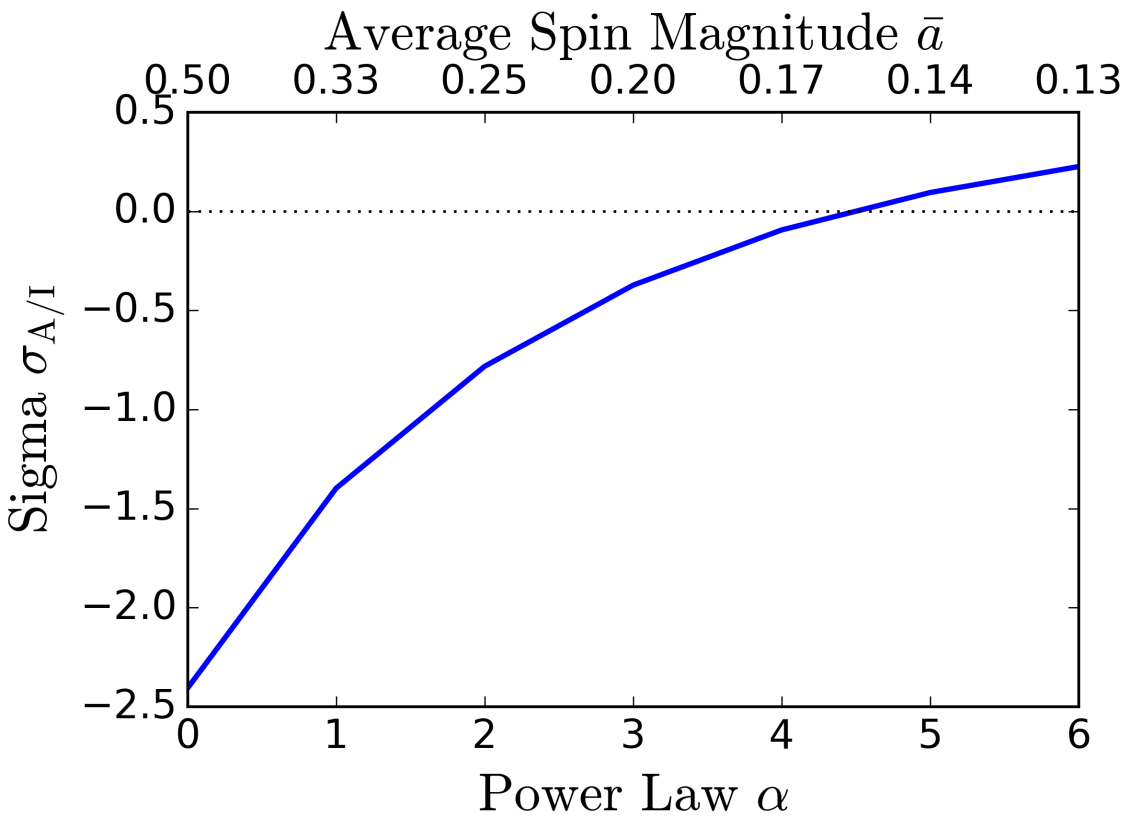

Figure 6. Effect of small spins on evidence ratio of aligned against isotropic models. The blue line shows the evidence ratio (plotted as the equivalent sigma) between a model where all systems are aligned, versus one where all systems are from an isotropic distribution as a function of the power law α corresponding to Equation C5. The top axis shows the mean spin magnitude $\bar{a}$ which this α corresponds to. We see that for mean spin magnitudes $\lesssim 0.2$ we find no evidence for either distribution over the other.

D. MASS RATIO

Figure 7 shows the distributions of $\chi_{\rm eff}$ that would obtain with a mass ratio $q = m_2/m_1 = 0.5$ compared to the distributions with $q = 1$ used above. The details of the distribution are sensitive to the mass ratio, but in our analysis we are primarily sensitive to the changing *sign* of $\chi_{\rm eff}$ under the isotropic models. This latter property is insensitive to mass ratio. As an example, the distinction between the three different spin amplitude distributions after ten additional detections is quite weak compared to the aligned/isotropic distinction in Figure 4. The differences in the $\chi_{\rm eff}$ distribution between $q = 1$ and $q = 0.5$ are even smaller than the differences between the different magnitude distributions.

E. APPROXIMATIONS IN THE GRAVITATIONAL WAVEFORM

The model waveforms used to infer the $\chi_{\rm eff}$ of the three LIGO events incorporate approximations to the true behaviour of the merging systems that are expected to break down for sufficiently high mis-aligned spins. The effect of these approximations on inference on the parameters describing GW150914 has been investigated in detail

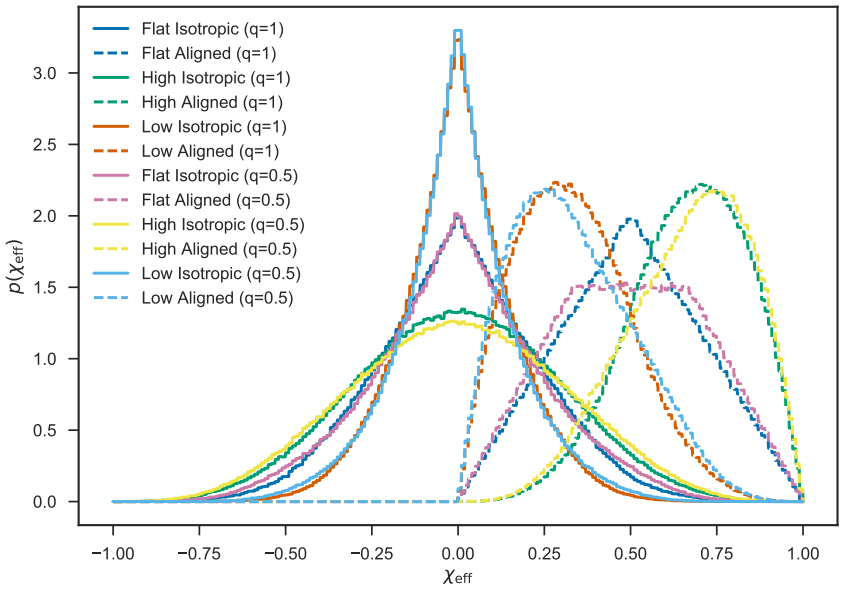

Figure 7. Distributions of $\chi_{\rm eff}$ assuming all merging black holes have equal masses ($q = 1$) or a 2:1 mass ratio ($q = 0.5$). The details of the distribution are sensitive to the mass ratio, but in our analysis we are primarily sensitive to the changing *sign* of $\chi_{\rm eff}$ under the isotropic models. This latter property is unchanged under changing mass ratio.

(Abbott et al. 2016f). For this source, statistical uncertainties dominate over any waveform systematics. Detailed comparisons with numerical relativity computations using no approximations to the dynamics (Abbott et al. 2016g) also suggest that statistical uncertainties dominate the systematics for this system. Abbott et al. (2016f) suggests that systematics may dominate for signals with this large SNR ($\simeq 23$) when the source is edge-on or has high spins. The other two events discussed in this paper are at much lower SNR, with correspondingly larger statistical uncertainties, and are probably similarly oriented and with similarly small spins, so we do not expect systematic uncertainties to dominate.

We assume here that measurements made in the future are not dominated by systematic errors, but this assumption would need to be revisited for high-SNR, edge-on, or high-spin sources detected in the future.

REFERENCES

Abbott, B. P., Abbott, R., Abbott, T. D., et al. 2016a, Physical Review Letters, 116, 241102

—. 2016b, Physical Review X, 6, 041015

—. 2016c, Physical Review Letters, 116, 241103

—. 2016d, ApJL, 833, L1

—. 2016e, ApJS, 227, 14

—. 2016f, ArXiv e-prints, arXiv:1611.07531

—. 2016g, PhRvD, 94, 064035

Albrecht, S., Reffert, S., Snellen, I. A. G., & Winn, J. N. 2009, Nature, 461, 373

Albrecht, S., Winn, J. N., Torres, G., et al. 2014, ApJ, 785, 83

Belczynski, K., Holz, D. E., Bulik, T., & O'Shaughnessy, R. 2016, Nature, 534, 512

Bogdanović, T., Reynolds, C. S., & Miller, M. C. 2007, ApJL, 661, L147

Farr, W. M., Kremer, K., Lyutikov, M., & Kalogera, V. 2011, ApJ, 742, 81

Fishbach, M., Holz, D., & Farr, B. 2017, ArXiv e-prints, arXiv:1703.06869

Fragos, T., & McClintock, J. E. 2015, ApJ, 800, 17

Gerosa, D., & Berti, E. 2017, ArXiv e-prints, arXiv:1703.06223

Gerosa, D., Kesden, M., Berti, E., O'Shaughnessy, R., & Sperhake, U. 2013, PhRvD, 87, 104028

Gerosa, D., Kesden, M., Sperhake, U., Berti, E., & O'Shaughnessy, R. 2015, PhRvD, 92, 064016

Hannam, M., Schmidt, P., Bohé, A., et al. 2014, Physical Review Letters, 113, 151101

Hogg, D. W., Myers, A. D., & Bovy, J. 2010, ApJ, 725, 2166

Hotokezaka, K., & Piran, T. 2017, ArXiv e-prints, arXiv:1702.03952

Kalogera, V. 2000, ApJ, 541, 319

King, A. R., & Kolb, U. 1999, MNRAS, 305, 654

Kulkarni, S. R., Hut, P., & McMillan, S. 1993, Nature, 364, 421

Kushnir, D., Zaldarriaga, M., Kollmeier, J. A., & Waldman, R. 2016, MNRAS, 462, 844

Lipunov, V. M., Postnov, K. A., & Prokhorov, M. E. 1997, MNRAS, 288, 245

Mandel, I. 2010, PhRvD, 81, 084029

Mandel, I., & de Mink, S. E. 2016, MNRAS, 458, 2634

Marchant, P., Langer, N., Podsiadlowski, P., Tauris, T. M., & Moriya, T. J. 2016, A&A, 588, A50

Martin, R. G., Reis, R. C., & Pringle, J. E. 2008a, MNRAS, 391, L15

Martin, R. G., Tout, C. A., & Pringle, J. E. 2008b, MNRAS, 387, 188

Miller, M. C., & Miller, J. M. 2015, PhR, 548, 1

Morningstar, W. R., & Miller, J. M. 2014, ApJL, 793, L33

Orosz, J. A., Kuulkers, E., van der Klis, M., et al. 2001, ApJ, 555, 489

Pan, Y., Buonanno, A., Taracchini, A., et al. 2014, PhRvD, 89, 084006

Podsiadlowski, P., Rappaport, S., & Han, Z. 2003, MNRAS, 341, 385

Portegies Zwart, S. F., & McMillan, S. L. W. 2000, ApJ, 528, L17

Rodriguez, C. L., Morscher, M., Pattabiraman, B., et al. 2015, Physical Review Letters, 115, 051101

Rodriguez, C. L., Zevin, M., Pankow, C., Kalogera, V., & Rasio, F. A. 2016, ApJL, 832, L2

Schnittman, J. D. 2004, PhRvD, 70, 124020

Sigurdsson, S., & Hernquist, L. 1993, Nature, 364, 423

Stevenson, S., Berry, C. P. L., & Mandel, I. 2017a, ArXiv e-prints, arXiv:1703.06873

Stevenson, S., Vigna Gomez, A., Mandel, I., et al. 2017b, Nature Communications, in press

Stone, N. C., Metzger, B. D., & Haiman, Z. 2017, MNRAS, 464, 946

Taracchini, A., Buonanno, A., Pan, Y., et al. 2014, PhRvD, 89, 061502

Tutukov, A., & Yungelson, L. 1973, Nauchnye Informatsii, 27, 70

Tutukov, A. V., & Yungelson, L. R. 1993, Monthly Notices of the Royal Astronomical Society, 260, 675

Veitch, J., Raymond, V., Farr, B., et al. 2015, PhRvD, 91, 042003

Vitale, S., Lynch, R., Sturani, R., & Graff, P. 2017, Classical and Quantum Gravity, 34, 03LT01

Zaldarriaga, M., Kushnir, D., & Kollmeier, J. A. 2017, ArXiv e-prints, arXiv:1702.00885